Sensor Network Design for Maximizing Process Efficiency: An Algorithm and Its Application

Prokash Paul, Debangsu Bhattacharyya, and Richard Turton
Dept. of Chemical Engineering, West Virginia University, Morgantown, WV 26506

Stephen E. Zitney
U.S. Dept. of Energy, National Energy Technology Laboratory, Morgantown, WV 26507

DOI 10.1002/aic.14649
Published online October 30, 2014 in Wiley Online Library (wileyonlinelibrary.com)

Sensor network design (SND) is a constrained optimization problem requiring systematic and effective solution algorithms for determining where best to locate sensors. A SND algorithm is developed for maximizing plant efficiency for an estimator-based control system while simultaneously satisfying accuracy requirements for the desired process measurements. The SND problem formulation leads to a mixed integer nonlinear programming (MINLP) optimization that is difficult to solve for large-scale system applications. Therefore, a sequential approach is developed to solve the MINLP problem, where the integer problem for sensor selection is solved using the genetic algorithm while the nonlinear programming problem including convergence of the "tear stream" in the estimator-based control system is solved using the direct substitution method. The SND algorithm is then successfully applied to a large scale, highly integrated chemical process. © 2014 American Institute of Chemical Engineers *AIChE J*, 61: 464–476, 2015
Keywords: sensor placement, estimator-based control system, efficiency maximization, parallel computation, integrated gasification combined cycle, acid gas removal unit

Introduction

Sensor networks play an important role in plant operation, control, and monitoring. However, it is difficult to select the number, location, and type of sensors for systematically designing an optimal plant-wide sensor network. The optimal sensor network design (SND) strongly depends on the objective(s) and constraints considered for sensor placement. Some of the common objectives for SND are maximizing the estimation accuracy, minimizing the sensor network cost, maximizing reliability, and maximizing robustness. Some of the typical constraints are desired level of precision, reliability, estimability of key variables, sensor network cost being lower than some budget, and/or desired level of robustness of the sensor network. Depending on the underlying SND problem, the approaches and solution algorithms vary greatly. It should be noted that SND algorithms can also be developed from a fault diagnosis perspective; although this is not the focus of this study.

SND has been an area of active research for the past several decades and a review up to year 2000 can be found in the book by Bagajewicz.[1] Usually, a sensor network is designed either for fault detection and identification or process monitoring purposes. Fault diagnosis is beyond the scope of this article, interested readers are referred to some of the seminal works in SND by Raghuraj et al.,[2] Bhushan and Rengaswamy,[3–6] Musulin et al.,[7] and Narasimhan and Rengaswamy.[8] One of the popular goals for SND is to obtain the cost-optimal sensor network. Bagajewicz et al.[9–11] and Chmielewski et al.[12] obtained a minimal cost SND subject to constraints on precision, error detectability, reliability, and resilience. Kelly and Zyngier[13] minimized the cost of a sensor network with constraints on software and hardware redundancy of the measured variables and constraints on the observability and precision of the unmeasured variables. From the data reconciliation perspective, Kretsovalis and Mah[14] used estimation accuracy for SND at minimal cost. The authors showed that redundancy in measurements improved the estimation accuracy. Kadu et al.[15] considered the effect of different sampling frequencies on state estimation accuracy and developed a methodology to solve an implicit multiobjective optimization problem. Conversely, Madron and Veverka[16] adopted a Gauss–Jordan elimination method for achieving observability of all key variables at the minimum cost of the sensor network. Ali[17–19] considered

Disclaimer: This project was funded by the Department of Energy, National Energy Technology Laboratory, an agency of the United States Government, through a support contract with URS Energy & Construction, Inc. Neither the United States Government nor any agency thereof, nor any of their employees, nor URS Energy & Construction, Inc., nor any of their employees, makes any warranty, expressed or implied, or assumes any legal liability or responsibility for the accuracy, completeness, or usefulness of any information, apparatus, product, or process disclosed, or represents that its use would not infringe privately owned rights. Reference herein to any specific commercial product, process, or service by trade name, trademark, manufacturer, or otherwise, does not necessarily constitute or imply its endorsement, recommendation, or favoring by the United States Government or any agency thereof. The views and opinions of authors expressed herein do not necessarily state or reflect those of the United States Government or any agency thereof.

Correspondence concerning this article should be addressed to D. Bhattacharyya at Debangsu.Bhattacharyya@mail.wvu.edu.

maximization of estimation reliability as the objective of their SND algorithm and estimated reliability using the information on sensor failure probability. Peng and Chmielewski[20,21] placed the sensors based on a controls perspective and also gave simultaneous formulation of sensor selection and minimal backed-off operating point selection by maximizing the operating profit.

SND from an economic perspective has been carried out by Bagajewicz et al.[22,23] where the authors have obtained an expression for assessing the value of precision. Later Bagajewicz[24] extended the economic value of precision by introducing the effect of induced bias obtained by evaluating the economic value of accuracy. Bagajewicz and coworkers[25–27] have also investigated economic value of data reconciliation and instrumentation upgrades. Nabil and Narasimhan[28] proposed SND based on the loss of operational profit caused by measurement uncertainty and solved a mixed integer cone problem to obtain a globally optimal sensor network.

Different computational methods have been used in the exiting literature to solve the SND problem. Chmielewski et al.[12] used a branch and bound algorithm to find the global optimum solution. Nguyen and Bagajewicz[29,30] used an equation-based tree search method for medium-scale nonlinear problems to obtain global optimal solution of an SND problem for process monitoring purposes. A graph-theoretic method was used by Meyer et al.[31] and Luong et al.[32] to design a sensor network for process monitoring. Zumoffen and Basualdo[33] used a genetic algorithm (GA) to achieve an efficient monitoring system for large-scale chemical plants. Carnero et al.[34,35] used GA for the optimal design of nonredundant observable linear sensor networks. Combined concepts of graph theory and GA are used by Sen et al.[36] to optimize a single criterion of cost, reliability, or estimation accuracy. Lee and Diwekar[37] presented a novel approach for optimal SND under uncertainty in an integrated gasification combined cycle (IGCC) power plant using Fisher information as a metric for observation order. Recently, Nguyen and Bagajewicz[38] have proposed an SND algorithm for maximizing the difference between the economic value of information and cost. The authors have solved the SND problem using GA.

To the best of our knowledge, there is no SND algorithm in the existing literature for maximizing process efficiency. If an estimator-based control system is considered, the measurements from the sensor network pass through the estimator, and the controllers take action based on the estimated values. This, in turn, affects the process and, therefore, the measured variables. This continues until the process reaches its new steady state. It should be noted that for an estimator-based control system, the feedback error signal calculated with respect to the estimated value of the controlled variables has to go to zero at the steady state. Therefore, the error calculated with respect to the true value of the controlled variables is not necessarily zero and depends on the estimation error. As the estimation accuracy of some of the controlled variables (this point will be explained in the following paragraphs) can affect the efficiency of the process, the sensor network can impact the process efficiency. In addition, the feedback control loop affects the estimation accuracy of other key process variables that are used for monitoring purposes. The feedback loops are difficult to consider in the SND algorithm as the impact of the feedback control loops in the presence of an estimator-based control system should be taken into account while evaluating the objective for SND and checking for constraint violation. It should be noted that most SND algorithms have been developed without considering the effect of the feedback loop on the process efficiency in an estimator-based control system.

The variables measured by sensors in the plant can be of two types. The first type is used for monitoring purposes. For example, if the measured variable is an environmental variable, then a measurement error can lead to violation of environmental emission limits. Furthermore, if the measured variable is a key variable for monitoring the health of an equipment item, an error can lead to undesired conditions such as equipment damage. In addition, many other process variables are monitored to avoid safety hazards, or unwanted products, or other undesired conditions. Therefore, desired estimation accuracy must be achieved by the measurement network for these variables. It should be noted that if a variable is measured only for monitoring purposes and no (control) action is taken based on that measurement, the plant operation is not affected due to this type of variable.

The second type of measured variable is used as a controlled variable. Some variables under this category can affect the plant efficiency. For example, the liquid level in the sump of a distillation tower has minimal impact on the plant efficiency under perfect control. The controlled variables that affect plant efficiency may be known to a user due to past experiences or can be determined experimentally or through process simulations by evaluating the sensitivity of process efficiency with respect to a particular process variable. If the plant control structure has been systematically designed by optimizing its economic performance by following a method similar to that proposed by Skogestad[39] and further extended by Jones et al.,[40] then all primary controlled variables in such control structures affect the plant efficiency. It can be noted that in the method proposed by Skogestad,[39] the primary controlled variables are selected through steady-state economic analysis.

Jones et al.[40] have extended the work of Skogestad[39] by incorporating the control performance of the primary controlled variables in the selection criteria. In this approach, optimizations are performed for maximizing an economic objective with respect to steady-state degrees of freedom (DOF) by considering various disturbances. The active constraints are selected as primary controlled variables. In addition, depending on the remaining DOF, additional controlled variables are selected so that they are self-optimizing. The self-optimizing controlled variables are those that when left constant result in an acceptable economic loss in the face of disturbances.[41] If the primary controlled variables in a plant are self-optimizing and the plant has been optimally designed, then a deviation from the optimal values of the controlled variables would result in a loss in efficiency. The extent of this loss in efficiency depends on the magnitude and direction of the deviation. A low estimation accuracy of these variables will lead to a loss in efficiency. Conversely, setting an arbitrarily high estimation accuracy will result in undesired increase in the cost of the senor network. Therefore, unlike existing SND methods where the desired estimation accuracy of all variables of interest is set by the user, no specifications are needed for estimation accuracy of the self-optimizing controlled variables when using the estimator-based control system.

Conversely, for the primary controlled variables that are active constraints, the change in the process efficiency with respect to a change in the variable is monotonic, at least

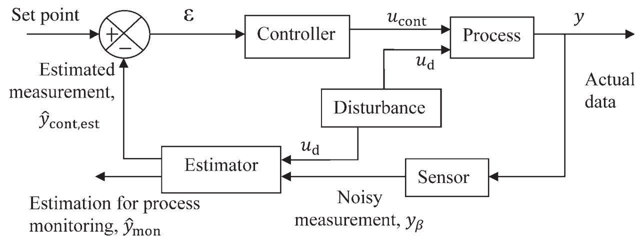

Figure 1. Schematic of the estimator-based control system for development of the SND algorithm.

locally. Therefore, specifications have to be provided by the user for either the positive or the negative estimation accuracy of these variables but not for both positive and negative. This aspect is better explained by the following example. Consider a CO_2 capture unit with an operational objective of 90% CO_2 capture. It has been well documented that CO_2 capture can strongly affect plant efficiency.[42] Due to inaccuracies in the measurement system, two undesired operational scenarios with regards to maintaining the target capture rate may occur. In the first scenario, the measurement system might show that CO_2 capture is less than the target (e.g., 89.8%) even though the actual capture is exactly 90%. In this scenario, the plant operators/control system will change the operating conditions to increase the amount of CO_2 capture to maintain it at the set point thereby causing a loss in process efficiency. For this scenario, the negative estimation accuracy can be determined by considering the trade-off between efficiency and cost. In the second scenario, if the measurement system shows a greater (i.e., 90.2%) CO_2 capture level even though the actual capture is 90%, the plant operators/control system will change the operating conditions to decrease the CO_2 capture. As a result more CO_2 will be released to the environment, which can result in a penalty from the regulating agencies. For this scenario, the allowable positive estimation accuracy has to be set by the user. For many measurement instruments, the estimation accuracy guaranteed by the manufacturer is the same in both positive and negative direction. For such instruments, the SND algorithm should automatically determine the limiting deviation and design the sensor network accordingly.

With these motivations and the background provided above, a new SND algorithm has been developed assuming an estimator-based control system where an optimal Kalman filter (KF)[43] is used to estimate the states in the presence of measurement and process noise. Due to the feedback loop in the control system, the resulting system of equations becomes very difficult to converge for any arbitrary set of integer variables (i.e., set of sensors). A sequential optimization algorithm is developed that follows the infeasible path method where a "tearing" approach is used to solve the feedback loops. The methodology is developed in a way that large-scale systems can be solved efficiently. As mentioned before, this algorithm does not require the user to provide an estimation accuracy for the self-optimizing controlled variables unless the user desires to do so for some specific reason. For example, if a chemical plant emits H_2S to the environment and its composition in the emission gas is the self-optimizing controlled variables, then estimation accuracy must be provided for H_2S capture. For the controlled variables that are active constraints, only one estimation accuracy, either positive or negative, has to be provided by the user. For all other variables that are used for monitoring purposes, the desired estimation accuracy has to be provided by the user.

In this work, the integer programming (IP) problem is solved by GA while other linear and nonlinear constraints are satisfied by a sequential equation solver using a "tear" stream approach. As discussed below in more detail, this formulation helps in satisfying the linear and nonlinear equality constraints for every combination of integer variables.

Many of the SND algorithms in the existing literature have been applied to small simplified test problems. In this work, the developed methodology is applied to a large, high-integrated acid gas removal (AGR) unit as part of an IGCC power plant with CO_2 capture. This AGR unit comprises of a number of typical unit operations involving considerable mass and energy integration and, therefore, is a very good industrial case study for the proposed algorithm.

This following organization is adopted in this article. First, the SND algorithm for efficiency maximization for an estimator-based control system is developed. This is followed by a discussion of the solution approaches to the SND problem. Finally, the application of the SND algorithm to the AGR case study is presented.

Development of the SND Algorithm

Figure 1 shows the estimator-based control system that is used to develop the SND algorithm. Perturbed by a disturbance, u_d, the estimator receives the noisy measurements, y_β, from the sensor network and estimates the process variables of interest for use in control $(\hat{y}_{\text{cont,est}})$ and monitoring $(\hat{y}_{\text{mon}})$. The controller(s) then implement(s) the corrective action on the process based on the estimated controlled variables.

For developing the SND algorithm, first the set of equations corresponding to each block of the estimator-based control system is organized. The estimator block in Figure 1 is considered to be a continuous KF. The process and measurement models are given by the following equations

$$\frac{dx_{\text{act}}}{dt}=Ax_{\text{act}}+Bu+w \tag{1}$$

$$y=Cx_{\text{act}}+v \tag{2}$$

In Eq. 1, A $(n\times n)$ and B $(n\times m)$ are the constant nonsingular transition matrix and input matrix, respectively. Equation 2 defines the relationship between the measurement vector (y) and the state vector (x_{act}). C $(l\times n)$ is the measurement matrix. The mismatch between the nonlinear process and the linear state-space model is captured by the random variable w, typically known as the process noise vector. The random variable v in Eq. 2 represents measurement noise. Process noise (w) and measurement noise (v) are assumed to be uncorrelated, Gaussian, white noise sequences with zero-mean.

An optimal KF[43] is used to estimate the states and disturbances of the process. Table 1 shows the equations that characterize the closed-loop blocks: estimator, comparator, and controller. Linear differential equations (Eq. 3) are used to estimate the states $\hat{x}$ of the controlled variables and other key performance variables of the process in the presence of noisy measurements, y and Kalman gain, K. Kalman gain can be obtained by first integrating the nonlinear matrix differential Riccati equation (Eq. 4) for the state covariance matrix, P, and then solving the matrix equation (Eq. 5) for the Kalman gain. Q is the process noise variance-covariance

Table 1. Equations Characterizing the Estimator, Comparator and Controller Block (in Figure 1)

Estimator (KF)		Comparator	
$\frac{d\hat{x}}{dt}=A\hat{x}+Bu+K(y-C\hat{x})$	(3)	Estimated measurements: $\hat{y}_{\text{cont,est}}=C_{\text{cont}}\hat{x}$	(8)
$\frac{dP}{dt}=-PC^{\text{T}}R^{-1}CP+PA^{\text{T}}+AP+Q$	(4)		
$K=PC^{\text{T}}R^{-1}$	(5)	Error function: $\varepsilon(t)=y_{\text{cont,set}}-\hat{y}_{\text{cont,est}}$	(9)
$Q=E[ww^{\text{T}}]$	(6)	Controller (proportional-only)	
$R=E[vv^{\text{T}}]$	(7)	Control action: $\frac{du_{\text{cont}}}{dt}=K_{\text{c}}\frac{d\varepsilon(t)}{dt}$	(10)

matrix that is related to the process noise column vector (w) in Eq. 6. Similarly, the measurement noise variance-covariance matrix R consists of spectral densities describing the measurement noise, v, in Eq. 7. Usually, Q and R are used as tuning parameters. They are either manually tuned or kept constant during state estimation. As the tuning parameters are unknown, a good guess is crucial for both of them.

The comparator receives the estimated measurements (Eq. 8) and compares them with the set point of the controlled variables of interest and calculates the error functions, $\varepsilon(t)$ (Eq. 9). In this case, a proportional-only (P) controller has been assumed mainly for simplicity. Equation 10 shows the time variant proportional control action, where K_{c} is the proportional gain.

For simplicity and reduction of computational expense, the SND algorithm is developed under steady-state assumptions. In addition to the steady-state versions of the equations shown in Table 1, the inequality constraints shown in Eqs. 11 and 12 are also considered. In Eq. 11, parameter b denotes the budget ($) for the sensor where the left side of the inequality represents total cost of placed sensors for obtaining measurements and c_i denotes the cost of individual sensor i.

$$\sum_{\forall i} c_i\beta_i \le b \quad \forall i \in N_{\text{s}} \tag{11}$$

$$|y_{\text{ma,act}}-C_{\text{ma}}\hat{x}| < \text{tol}_1 \tag{12}$$

β_i takes on a value of 1 if a sensor is placed to measure the process variable, otherwise it is 0. In Eq. 12, tol_1 is the tolerance limit vector on the estimation error and the left side of the inequality is the vector of actual minus vector of estimated value $(C_{\text{ma}}\hat{x})$ of process monitoring variables as well as active constraints. The objective function is defined as the deviation of the actual efficiency of the plant from the optimal efficiency. The optimal efficiency, η_{opt}, is the maximum efficiency when the plant runs under optimal operating conditions with no estimator and measurement errors. Therefore, η_{opt} is the maximum efficiency that can be attained. The efficiency of the process in the presence of estimator-based control system is denoted by $\eta(x_{\text{act}},\beta)$. It should be noted that one down-side of the steady-state assumption is that the KF is essentially being used to estimate steady-state bias.

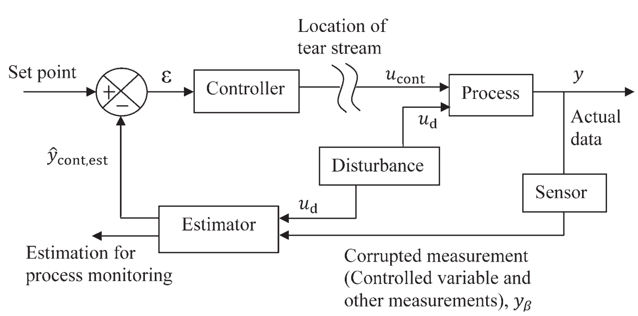

Figure 2. Sequential solution approach to the SND problem for the estimator-based control system.

The SND objective is to maximize $\eta(x_{\text{act}},\beta)$ for a given budget for sensors. This is equivalent to the minimization of the squared error between the maximum efficiency and the actual efficiency of the plant with the sensors in place. Therefore, after some substitutions and rearrangement, the SND problem is given by

$$\left.\begin{aligned}
&\text{Min}(\eta_{\text{opt}}-\eta(x_{\text{act}},\beta))^2\\
&\text{s.t.}\\
&Ax_{\text{act}}+Bu+w=0\\
&C_\beta=[C_{ij}]_{\beta_i\neq 0};\quad v_\beta=[v_i]_{\beta_i\neq 0}\\
&i=1,2,\dots\dots l;\quad j=1,2,\dots\dots n\\
&y_\beta=C_\beta x_{\text{act}}+v_\beta\\
&AP+PA^{\text{T}}-PC_\beta^{\text{T}}R_\beta{}^{-1}C_\beta P+Q=0\\
&K=PC_\beta^{\text{T}}R_\beta{}^{-1}\\
&A\hat{x}+Bu+K(y_\beta-C_\beta\hat{x})=0\\
&\sum\nolimits_{\forall i} c_i\beta_i \le b\\
&\beta_i=0,1 \quad \forall i\in N_{\text{s}}\\
&|y_{\text{ma,act}}-C_{\text{ma}}\hat{x}| < \text{tol}_1
\end{aligned}\right\} \tag{13}$$

N_{s} is the set of all candidate sensors. In this formulation, the variable y in Eq. 2 is replaced by y_β as the set of available measurements. C_β is the measurement matrix of the available sensors and the corresponding measurement noise is v_β. It should be noted that β is the set of integer variables while the remaining variables are continuous. Therefore, the SND is a mixed integer nonlinear programming (MINLP) problem which can be solved by two solution approaches: a simultaneous solution approach or a sequential solution approach.

Simultaneous Solution Approach

In the simultaneous approach, all the constraints are satisfied at the same time. However, the developed algorithm has a large number of variables including the actual states, outputs, estimated states, and the elements of the state covariance matrix, P. If there are n state variables and $\sum\beta_i$ integer variables, then the total number of continuous and integer variables in the SND problem is $2n+2\sum\beta_i$. In addition, the solution of $n\times n$ matrix Riccati equations and computation of steady-state Kalman gain matrix of identical dimension results in extensive computational complexity. In the case of a very large size problem involving more than a thousand states, this approach becomes computationally very expensive. Furthermore, it becomes very difficult to make an

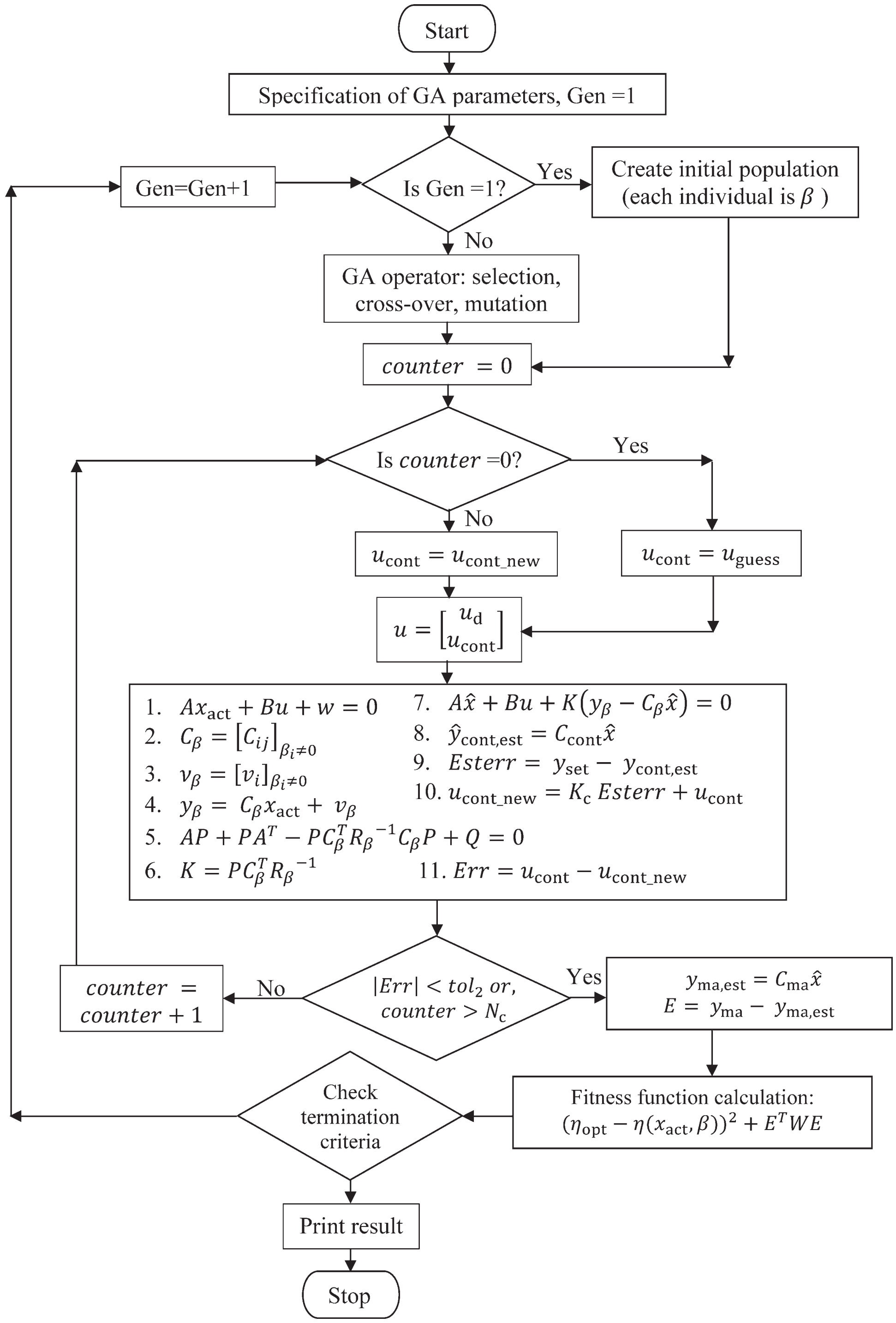

Figure 3. Algorithm to simulate feedback control system with an estimator.

initial guess for the continuous variables, especially for P for every possible combination of integer variables (i.e., selected sensors). A bad initial guess can result in high computation expense and in the worst case can lead to failure. One typical approach to solve the MINLP problem is to separate the IP problem from the nonlinear programming (NLP) problem. But again, the convergence of the NLP problem is extremely difficult because of the reason mentioned above. Based on our extensive testing of a number of case studies, this approach is found to be suitable for small problems with very few states and candidate sensor locations. As our objective is to apply the SND algorithm to large systems, this approach was not pursued further. Instead, a sequential modular approach described in the following section is developed.

Sequential Solution Approach

In this approach, the MINLP problem for SND is solved by solving the IP problem by GA while the NLP problem is solved sequentially as described below. The proposed sequential approach is similar to the sequential modular approach used for solving process flow sheeting problems. In

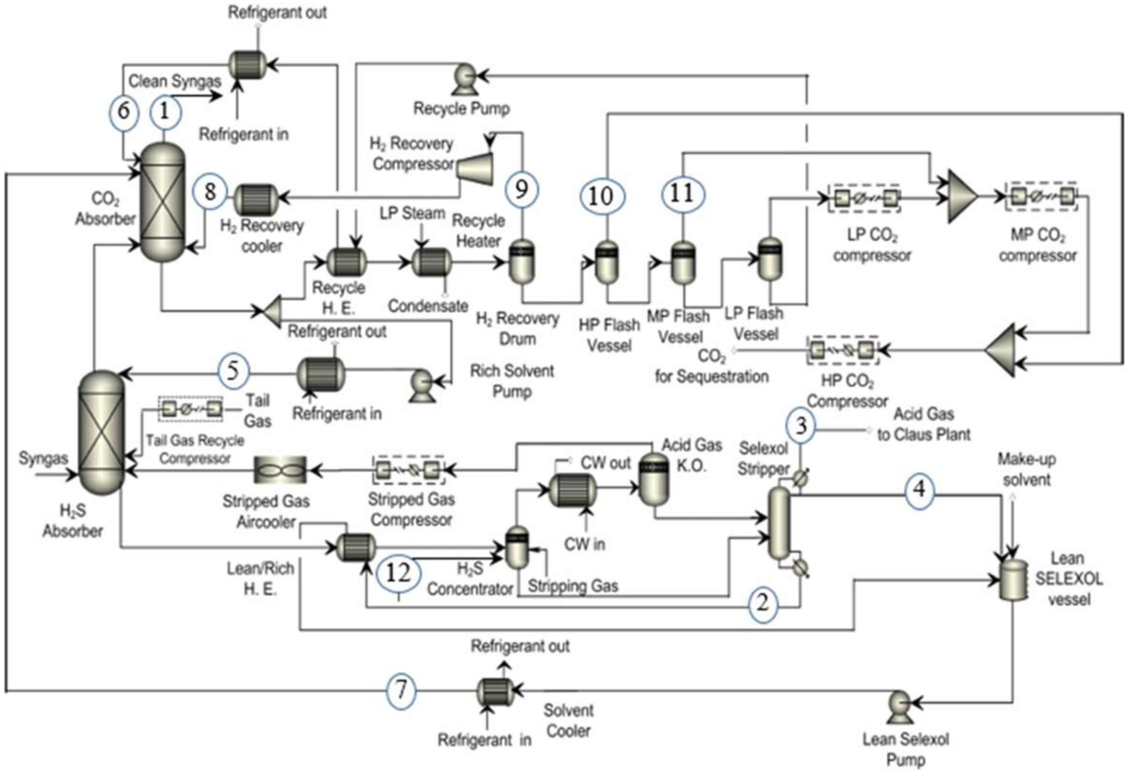

Figure 4. Configuration of the AGR and CO_2 compression units.[45]

[Color figure can be viewed in the online issue, which is available at wileyonlinelibrary.com.]

this approach, each estimator-based control loop is opened by tearing a stream and then the blocks are solved sequentially until a convergence criterion is satisfied. The proposed approach is shown in Figure 2. Although the tear-stream location can be any location such that the loop is opened, the location chosen in this work, as shown in Figure 2, helps to reduce the total number of tear variables and helps to generate initial guesses for the tear variables (i.e., the inputs).

As the NLP problem is solved sequentially, the objective function in the GA is modified to introduce the penalty term for the estimation error in the process monitoring variables and active contraints. Figure 3 shows the algorithm for the sequential solution approach.

The SND algorithm is developed under the assumption of perfect implementation of control action in the feedback control loop, that is, implementation error due to the actuator and any associated hardware/software is neglected. The developed algorithm is solved using GA. The flow sheet in Figure 3 starts with the specification of GA parameters and proceeds with the creation of an initial population in the first generation (denoted by Gen in Figure 3). Each solution set β in the population consists of decision variables, that is, locations of sensors. A counter is set to reduce the excessive computational time for those solution sets that fail to satisfy the convergence criterion. The estimator-based feedback control loop starts with counter=0 and an initial guess for the tear stream (u_{cont}). The initial guess is generated by considering the process model and assuming perfect control and measured disturbances. Input, u, is obtained by augmenting the disturbance vector, d, with u_{cont}. In Step 1, the process model is solved to calculate the actual states, x_{act}, using the augmented vector u. In Steps 2 and 3, those rows of the measurement matrix and measurement noise vector that correspond to $\beta_i=0$ (ith row) are rejected. As a result, the dimension of C_β and v_β reduces to $\sum\beta_i$ by n and $\sum\beta_i$ by 1, respectively. This is followed by Step 4, where noisy measurements are obtained using the linear algebraic measurement equations and adding measurement noise v_β. Step 5 involves solving the algebraic Riccati equation to obtain the process noise covariance matrix (P) followed by the calculation of the steady-state Kalman gain matrix (K) in Step 6. Once the steady-state gain is available, the estimated states, $\hat{x}$, can be computed in Step 7 that are then used in Step 8, to obtain estimated controlled variables, $\hat{y}_{\mathrm{cont,est}}$. In the Step 9, error is determined from the difference between the set point and the estimated controlled variables. Based on this error, in Step 10, the P-only controller computes necessary control action $u_{\mathrm{cont}_{\mathrm{new}}}$. Until $|\mathrm{Err}|$ satisfies the tolerance or the counter is less than the prespecified number for the iteration loop, the entire computation loop is repeated with the updated u_{cont}. It should be noted that when $|\mathrm{Err}|$ satisfies the tolerance and the tolerance is set at a low enough value, the solution represents the steady state of the entire system. The steady-state solution for a particular candidate set of sensors is achieved after a number of iterations. Then, the feasible candidate set is assigned a fitness value based on the objective function. The infeasible set of sensors that does not satisfy the estimation accuracy in monitoring variables as well as in active constraints penalizes the objective function by adding $E^{\mathrm{T}}WE$ where W is a weighting factor. The GA continues until the convergence criterion is satisfied.

The SND algorithm presented here uses the "direct substitution" method for tear-stream convergence. For highly interacting systems, other algorithms for tear-stream convergence such as Broyden's method or Newton's method might be necessary.

Table 2. List of Primary Controller Variables and Pairings

	Active Constraints		Manipulated Variables
1.	CO_2 capture	1.	Low pressure flash pressure
2.	Water content of solvent at stripper bottom	2.	Steam flow rate
3.	Stripper pressure	3.	Stripper vapor flow rate
4.	Stripper top temperature	4.	Stripper condenser duty
5.	Semi-lean solvent cooler outlet temperature	5.	Semi lean solvent cooler duty
6.	Loaded solvent cooler outlet temperature	6.	Loaded solvent cooler duty
7.	Lean solvent cooler outlet temperature	7.	Lean solvent cooler duty
8.	H_2 cooler outlet temperature	8.	H_2 cooler duty
	Self-optimizing Controlled Variables		Manipulated Variables
9.	Pressure of the H_2 recovery unit	9.	H_2 recovery outlet valve position
10.	Pressure of the HP flash vessel	10.	HP compressor brake power
11.	Pressure of the MP flash vessel	11.	MP compressor brake power
12.	N_2 flow rate to H_2S concentrator	12.	Valve opening of the N_2 feed valve

Genetic Algorithm

The GA is based on the principle of biological evolution.[44] GA creates the initial solution sets and ranks them according to their fitness value. Solution sets with higher fitness values survive and act as parents to produce children for the next generation. Breeding is performed based on the prespecified crossover, mutation, and selection criteria. Over successive generations, the population "evolves" toward an optimal solution. The proposed SND problem is very suitable for the GA because:

- The problem is a combinatorial optimization problem.
- The GA can handle the inequality constraints with mixed integer linear programming problem.
- The SND problem is expected to have many extrema and, therefore, a global search is necessary.

Case Study

This section illustrates the application of the proposed SND methodology to a large-scale chemical process unit, specifically a selective, dual stage, chilled Selexol™ solvent-based AGR unit. The AGR unit considered for our study is a part of an IGCC power plant with precombustion CO_2 capture described in Bhattacharyya et al.[45] Figure 4 shows the configuration of the AGR unit and subsequent CO_2 compression system.

The AGR process is dual stage and selective to both H_2S and CO_2 capture. Chilled solvent is used to remove H_2S in the first stage followed by a second stage that removes CO_2. Most of the H_2S in the syngas entering the AGR process is absorbed in the semi-lean solvent as it passes through the H_2S absorber. The tail gas from the Claus sulfur capture unit is recycled to the H_2S absorber. The off-gas from the top of the H_2S absorber is sent to the CO_2 absorber. A portion of the loaded solvent (about 30% in the base case) from the bottom of the CO_2 absorber is chilled and sent to the H_2S absorber. The remaining portion of the loaded solvent from the bottom of the CO_2 absorber is heated and then flows through the H_2 recovery drum. After that it goes through a series of three flash vessels, high pressure (HP), medium pressure (MP), and low pressure (LP), to recover CO_2 for compression in preparation for storage. The semi-lean solvent leaving the LP flash vessel is cooled by exchanging heat with the loaded solvent and is then chilled before returning to the CO_2 absorber. The rich solvent from the bottom of the H_2S absorber is heated and then sent to a flash vessel. The vapor from the flash vessel is recycled back to the H_2S absorber. The bottom stream from the flash vessel goes to the solvent stripper. Make-up solvent is mixed with the stripped solvent and sent to the top tray of the CO_2 absorber.

Table 3. List of Process Monitoring Variables

Constraint	Value
Maximum allowable solvent temperature	175°C
Minimum stripper pressure	276 kPa

For evaluating performance of AGR processes, usually measures such as $/tonne CO_2 captured or avoided is considered.[46] The dollar cost includes both operating and capital costs. From the sensor placement perspective, as we are mainly interested in the operating costs, amount of CO_2 captured per unit power consumption is considered to be the measure for efficiency of this AGR process. Thus, $\eta(x_{\mathrm{act}}, \beta)$ is defined for the AGR unit by the following equation

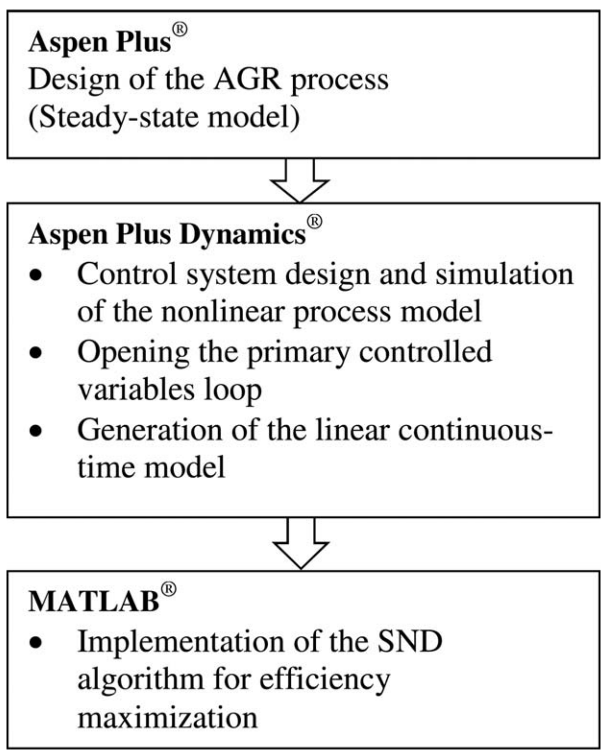

Figure 5. Workflow for implementation of the SND algorithm.

Table 4. Candidate Sensor Locations in the Equipment Items in the AGR Unit

Equipment	Sensors	No.
H_2S absorber	T_2, T_8, T_{14}, T_{20}, T_{26}, P_7, P_{16}, P_{25}, $(H_2S)_5$, $(H_2S)_{16}$, $(H_2S)_{25}$, $(CO_2)_5$, $(CO_2)_{16}$, $(CO_2)_{25}$	14
CO_2 absorber	T_2, T_8, T_{14}, P_3, P_9, P_{15},$(H_2S)_2$, $(H_2S)_8$, $(H_2S)_{14}$, $(CO_2)_2$, $(CO_2)_8$, $(CO_2)_{14}$	12
H_2S concentrator	T_3, T_5, P_4, $(H_2S)_1$, $(H_2S)_5$, $(CO_2)_1$, $(CO_2)_5$	7
Acid gas knockout	T, P	2
Solvent stripper	T_1, T_3, T_7, T_{10}, P_1, P_3, P_9, $(H_2S)_3$, $(H_2S)_9$, $(CO_2)_3$, $(CO_2)_9$	11
		Total = 46

$$\eta(x_{\text{act}}, \beta) = \frac{F_{CO_2,\text{in}}(x_{\text{act}}) - F_{CO_2,\text{out}}(x_{\text{act}})}{aF_{\text{solvent}}(x_{\text{act}}) + \sum_{c=1}^{3} P_c(x_{\text{act}})} \tag{14}$$

The numerator in Eq. 14 represents the amount of CO_2 captured while the denominator is the MWh power consumption. The variables in Eq. 14 are a function of x_{act} in the estimator-based control system.

The primary controlled variables for the AGR process have been identified by Jones et al.[40] and are shown in Table 2. An estimator-based control system has been implemented for active constraints and self-optimizing controlled variables as shown in Table 2. The interested reader is referred to Jones et al.[40] for details of the primary controlled variables and their selection method.

There are a number of operational constraints in the AGR unit considered as process monitoring variables and estimation accuracy must be satisfied for these variables. In this framework, it is easy to include more monitored variables for which estimation accuracy must be satisfied. However, in this case, for simplicity and testing, only two variables are considered for process monitoring purposes as shown in Table 3.

Figure 5 is the block diagram of the workflow based on the three different software platforms used, namely Aspen Plus® (AP), Aspen Plus Dynamics® (APD), and MATLAB®. AP® has been used to develop the steady-state process model of the AGR unit. The model is then exported to APD® for designing the control system and obtaining a stable dynamic model. Details about this model can be found in the works of Bhattacharyya et al.[45] and Jones et al.[40] Starting with this nonlinear process model of the AGR process in APD®, a continuous-time, linear model is generated by running a control design interface script that linearizes the nonlinear model around the steady-state operation conditions. All the primary controlled variable loops are kept open during the linearization of the model. The linear state-space model of the AGR unit, the algebraic measurement equations for candidate sensor locations, the primary controlled variables, and variables that appear in the objective functions are then exported to MATLAB®. It should be noted that even though all primary controlled variables have to be estimated by the measurement framework, sensors are not necessarily placed on all primary controlled variables. This is because measurement of some of these variables can be difficult and/or expensive and can have time delay, high noise, and/or low estimation accuracy. Conversely, it may be possible to estimate these variables satisfactorily by placing sensors elsewhere in the process and within the budget constraint. The optimal selection is done by the SND algorithm. In addition, satisfactory estimation of all other variable used for estimation purposes is desired. Therefore, the candidate sensor locations include other variables in addition to the primary controlled variables. The SND algorithm described above is implemented in MATLAB®.

The AGR process contains 1505 states. Two disturbances, including the change in the syngas flow rate and CO_2 concentration at the inlet of the AGR unit, have been considered. The flow rate disturbance is simulated by changing the inlet pressure of the syngas to the AGR unit. Four different types of commonly used sensors have been considered. These are temperature, pressure, flow, and composition (CO_2 and H_2S) sensors. They are denoted by T, P, F, y_{H_2S}, and y_{CO_2}, respectively, in the discussion below. The process flow sheet of the AGR unit is reviewed and the candidate sensor locations are identified based on the criteria mentioned below:

1. For columns including the H_2S and CO_2 absorbers, solvent stripper and H_2S concentrator, candidate T, P, y_{H_2S}, and y_{CO_2} sensor locations are shown in Table 4. As all columns are modeled using an equilibrium-stage assumption, temperatures of the liquid and vapor phases leaving a stage are the same. Therefore, only one T and P are considered for all these trays.
2. For the heat exchangers, T and P are measured at both inlet and outlet. As the mass/molar flow rate and composition does not change across the heat exchangers in the AGR unit, these variables are measured only at the outlet.
3. For each recycle stream, one flow meter is considered.
4. In all mixer blocks, no pressure drop has been considered. Therefore, T, F, y_{H_2S}, and y_{CO_2} vary, but P is constant.
5. For splitter blocks, F changes, but T, P, y_{H_2S}, and y_{CO_2} are constant.
6. Across the pump and valve, only P changes. There may be some changes in the temperature but that is neglected.
7. For compressors, both P and T change across the compressor.

After this analysis, 163 measurements are identified as potential locations for sensor placement. Tables 4 and 5 show the distribution of these candidate sensors in the AGR unit.

As mentioned before, P-only control has been considered in this work. It is required to obtain the tuning parameters of estimator-based controllers so that the closed-loop system in MATLAB® remains similar to the APD® model. The tuning parameter, in this case the proportional gain, is determined

Table 5. Candidate Sensor Locations in the Process Streams in the AGR Unit

Sensor Types	T	P	F	H_2S Analyzer	CO_2 Analyzer
No. of sensors	47	33	18	3	16
Total				117	

Table 6. Approximate Model Tuning Rules[49]

Tuning Rules	Controller Type	K_c
Ziegler–Nichols	Proportional controller	$\frac{1}{K_p}\left(\frac{\tau}{\alpha}\right)$
Cohen–Coon	Proportional controller	$\frac{1}{K_p}\left(\frac{\tau}{\alpha}\right)\left[1+\frac{1}{3}\left(\frac{\alpha}{\tau}\right)\right]$

Table 7. Tuning Parameters Used in the AGR Example

Primary Controlled Variables	K_p	τ (min)	α (min)	K_c (Ziegler–Nichols)	K_c (Cohen–Coon)
1. CO_2 capture	17.5	10.941	3.410	0.184	0.203
2. Water content of solvent at stripper bottom	0.128	66.136	0.457	1133	1135
3. Stripper pressure	0.102	0.355	0.060	57.863	61.125
4. Stripper top temperature	241	0.095	0.060	0.007	0.008
5. Semi lean solvent cooler outlet temperature	0.556	0.086	0.060	2.584	3.184
6. Loaded solvent cooler outlet temperature	1.726	0.088	0.060	0.854	1.047
7. Lean solvent cooler outlet temperature	11.362	0.077	0.060	0.112	0.142
8. H_2 cooler outlet temperature	72.6	0.108	0.060	0.025	0.029
9. Pressure of the H_2 recovery unit	0.162	5.870	0.432	83.967	86.027
10. Pressure of the HP flash vessel	0.017	3.808	0.543	403.373	422.6
11. Pressure of the MP flash vessel	0.019	3.415	0.496	353.757	370.9
12. N_2 flow rate to H_2S concentrator: F_{N_2}	115.853	0.238	0.060	0.0342	0.037

Note: Signs of K_p and K_c not shown.

Table 8. Cost of Sensors[50] Used in the AGR Example

Types		Range	Inaccuracy	\$ Cost Range	Cost Used
Flow sensor(plate + flanges + flanged meter + transmitter)	Gas phase	5–20 cm pipe	±0.25 to ±0.5% of actual flow	\$1500–3500	\$3400
	Gas phase	20–50 cm pipe		\$3500–8000	\$7000
	Liquid phase	1–35 cm pipe		\$1000–6000	\$5300
	Liquid phase	70–100 cm pipe		\$10,000–15,000	\$14,000
Pressure measurement device (integral with a transmitter)		0–6.9 MPa	0.1–1% of span	\$1500–3700	\$2500
Temperature (thermocouple integral with a transmitter)		−174.4 to 2337°C	±1 to ±2.8°C	\$700–2000	\$1000
H_2S analyzer (includes installation cost)		0–500 ppm	1% of full scale	\$65,000–145,000	\$70,000
CO_2 analyzer (explosion-proof NDIR analyzer with recorder, includes installation cost)		0–50 ppm	1–2% of full scale	\$10,000	\$10,000

using both Ziegler and Nichols[47] and Cohen and Coon[48] approximate model tuning rules. It can be noted that for the APD® model, the proportional-integral-derivative (PID) tuning parameters were obtained by Ziegler–Nichols and Cohen–Coon rules. In this case, the Ziegler–Nichols tuning rule outperforms the Cohen–Coon rule as latter one is more aggressive. The Ziegler–Nichols tuning rule is similar to the APD® model. Table 6 shows the rules that have been used to calculate the gain for the proportional controller.

Process gain (K_p), time constant (τ), and time delay (α) are obtained from the nonlinear process model in APD®. Table 7 presents the list of controllers and the corresponding tuning parameters obtained from the aforementioned tuning rules.

Table 9. Setup Parameters in GA

Parameters	
Generations	250
Selection	Stochastic uniform selection method
Crossover	Scattered crossover method
Population size	75
Mutation rate	0.01

As mentioned earlier, four types of sensors were considered: flow, pressure, temperature, and composition sensors. Flow sensors are further classified based on the phase of the stream and range of the flow rate. Table 8 shows the types of sensors, range, % inaccuracy, typical cost range, and the cost used in the work. The data provided in this table have

Table 10. Number of Sensors and the Value of the Objective Function for Different Budgets

Cases	Budget (Cost of Sensors, \$)	Number of Sensors	Efficiency (mol CO_2/MWh)	Computation Time
1	431,900	75	766.01	4 h 11 min
2	322,600	66	766.01	4 h 47 min
3	229,400	64	766.01	5 h 2 min
4	187,900	62	766.01	7 h 22 min
5	149,000	56	765.11	13 h
6	118,700	46	762.64	18 h
7	71,200	25	758.25	3 h 16 min
8	63,700	25	756.76	3 h 13 min
9	60,200	23	752.04	3 h 45 min
10	59,700	24	750.07	4 h 47 min
11	42,500	17	742.86	5 h 17 min

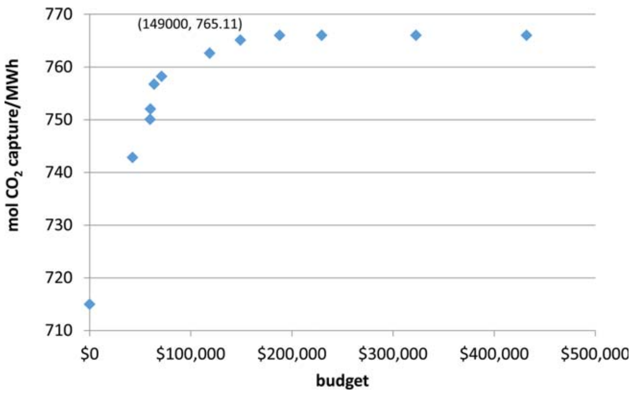

Figure 6. Objective function vs. cost of sensors.

[Color figure can be viewed in the online issue, which is available at wileyonlinelibrary.com.]

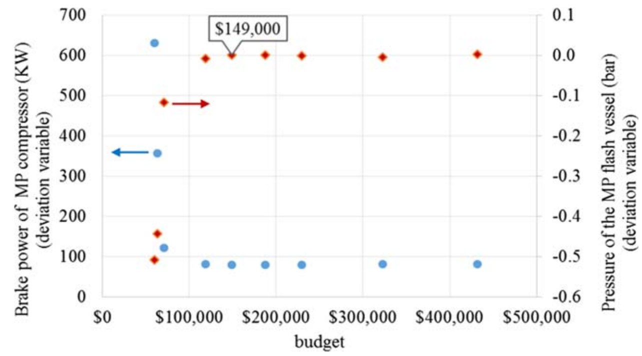

Figure 8. Manipulated variable: brake power of the MP CO_2 compressor (left); controlled variable: pressure of the MP flash vessel (right) against budget.

[Color figure can be viewed in the online issue, which is available at wileyonlinelibrary.com.]

been obtained from Liptak.[50] The cost of the sensors includes the price for measuring device, transmitter, other accessories as well as installation cost.

Due to the large size of the SND problem, considerable computational time is required to solve the constrained optimization problem on a single computer processor. For reducing the computation time, parallel computing was performed using the Distributed Computing Server (DCS®) and the Parallel Computing® toolbox from Mathworks®. The proposed algorithms were implemented in a MATLAB® program running on a computer cluster with 32 Intel®Xeon® 2.10 GHz processors with 64 GB RAM.

The methods for the GA operators and the values for the parameters are intuitively chosen in accordance with the scale of the problem using the guidelines provided in the literature.[44] Table 9 shows the key parameters in the GA specification.

Results

Efficiency of the AGR unit, defined as the amount of CO_2 capture per unit power consumption, is considered as the objective function in the SND algorithm. The maximum efficiency of the AGR unit as calculated from the dynamic model in APD® is 766.18 mol CO_2 capture/MWh when the plant runs under optimal operating conditions with no estimator and measurement errors. However, the value of the objective function without any measurements (i.e., estimator only) is the minimum value of the efficiency and is found to be 715.65 mol CO_2 capture/MWh. It is noted that the difference between the maximum and the minimum efficiency defined this way is a measure of the goodness of the process model.

Table 10 presents the results of some case studies for different budgets ($) for the sensor network. These case studies show that as the budget increases the number of sensors increases. Consequently, the number of available measurements also increases and/or costlier sensors are selected, which in turn can provide higher estimation accuracy for the process variables of interest as well as increased efficiency of the plant. Most of the CPU time is consumed for solving the matrix Riccati equation involving process covariance matrix of dimension 1505 × 1505. In addition, as this problem considers 163 potential sensor locations, a large combinatorial problem is solved for each budget constraint. The manuscript has been updated to include these informations. It is also observed from the case studies that the computational time depends on the initial population used by the GA. For the Cases 1–6, the computational time increases as the budget decreases. This is because of the higher number

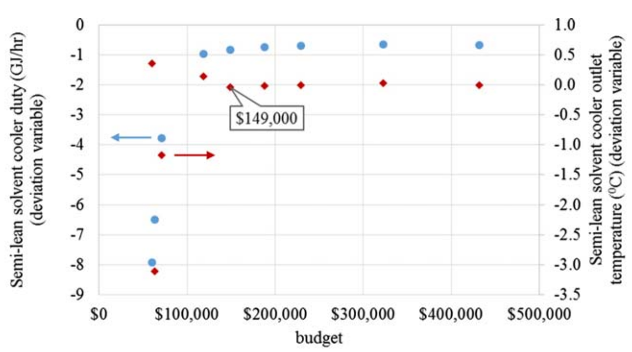

Figure 7. Manipulated variable: semi-lean solvent cooler duty (left); controlled variable: semi-lean solvent cooler outlet temperature (right) against budget.

[Color figure can be viewed in the online issue, which is available at wileyonlinelibrary.com.]

Figure 9. Manipulated variable: power of the HP compressor (left); controlled variable: pressure of the HP flash vessel (right) against budget.

[Color figure can be viewed in the online issue, which is available at wileyonlinelibrary.com.]

Table 11. Optimal Set of Sensors

	Temperature Sensor		Pressure Measuring Device
1.	H_2S absorber$_2$*	30.	H_2S absorber$_{16}$*
2.	H_2S concentrator$_5$*	31.	CO_2 absorber$_9$*
3.	Acid gas knockout drum vapor outlet	32.	Syngas cooler inlet
4.	CO_2 absorber$_8$*	33.	Off gas from top of H_2S absorber
5.	CO_2 absorber$_{14}$*	34.	Clean syngas at the top of CO_2 absorber
6.	Solvent stripper$_1$*	35.	Semi-lean solvent cooler inlet
7.	Solvent stripper$_3$*	36.	Rich solvent heater inlet
8.	Solvent stripper$_7$*	37.	Rich solvent at selexol stripper inlet
9.	Inlet to H_2O knockout drum	38.	Lean solvent at the inlet to CO_2 absorber
10.	Off gas from top of H_2S absorber	39.	Inlet to H_2 recovery flash vessel
11.	Off gas cooler outlet temperature	40.	H_2 recovery flash vessel
12.	Off gas at the inlet to CO_2 absorber	41.	Stripped gas compressor outlet
13.	Clean syngas at the top of CO_2 absorber	42.	Acid gas knockout drum liquid outlet
14.	Rich solvent at H_2S absorber bottom	43.	H_2 recovery compressor outlet
15.	Rich solvent heater inlet	44.	HP flash vessel outlet
16.	H_2 recovery flash vessel outlet	45.	Outlet of 1st LP CO_2 compressor
17.	HP flash vessel outlet	46.	Outlet of 2nd MP CO_2 compressor
18.	MP flash vessel outlet	47.	Glycol absorber top outlet
19.	Semi-lean solvent cooler inlet		Flow Sensor
20.	H_2S concentrator vapor outlet	48.	Semi-lean solvent to H_2S absorber
21.	Stripped gas compressor outlet	49.	H_2S concentrator vapor outlet
22.	First LP CO_2 compressor outlet	50.	H_2O K.O. drum bottom outlet
23.	Second LP CO_2 compressor outlet		CO_2 Analyzer
24.	Fifth LP CO_2 compressor outlet	51.	Liquid phase in H_2S absorber$_{16}$*
25.	First HP CO_2 compressor outlet	52.	Liquid phase in selexol stripper$_{16}$*
26.	First MP CO_2 compressor inlet	53.	H_2S absorber bottom
27.	Vapor of CO_2 flash vessel	54.	LP flash vessel bottom
28.	Liquid of CO_2 flash vessel	55.	Acid gas knockout drum liquid outlet
29.	Tail gas to H_2S absorber	56.	MP flash vessel vapor

*Subscript at the end of location denotes stage number.

of sensors that can be considered without violating the budget constraint. For the lower budget cases, that is, Cases 7–11, the initial population is created using the solution set of sensors obtained from the higher budget case studies. The computation time is significantly less for the lower budgets case studies. Using the DCS® and Parallel Computing® toolbox reduces the computation time by a factor of 6 compared to the nonparallel case studies.

Figure 6 shows how the optimal objective function value changes with the change in the budget. The figure shows that beyond \$149K budget (Case 5), the value of the objective function changes negligibly.

Figures 7–9 illustrate the underlying reason for the increase in efficiency as the budget for sensors increases. For brevity, the impact of the budget on the estimation accuracy of a few key input–output variables is presented. As the budget increases, the estimation accuracy of the controlled variables improves. As a result, the values of the manipulated variables approach the values that were obtained for the maximum efficiency case. The vertical axes denote deviation variables and are calculated with respect to the values that were obtained for the maximum efficiency case.

Figure 7 shows how the semi-lean solvent cooler duty changes with the increase in sensor cost. In the semi-lean solvent cooler, the NH_3-refrigerant is used for chilling the solvent. As shown on the right-hand side axis of Figure 7, for lower budgets, the estimate of the temperature at the outlet of the refrigeration cooler deviates more on the negative side, that is, it leads to a cooler temperature which is suboptimal. As a result, higher refrigeration duty is required at lower budget leading to loss in efficiency. Regardless of the noise in the measurements obtained from sensors, the estimated value of the controlled variable approaches to the optimal value as the sensors budget increases beyond \$149K as shown in Figure 7.

Figures 8 and 9 show how the compressor brake power changes as budget changes. Figures 8 and 9 show the brake power of the MP and HP CO_2 compressors, respectively. In both the cases, at lower budget, the estimated flash vessel pressures are lower than the optimal value. As a result, the compressors consume more power than the optimal case leading to decrease in the efficiency. As before, even in the presence of process and measurement noise, the estimated value of pressure approaches the optimal value as the sensors budget increases beyond \$149K (labeled in Figures 8 and 9).

Table 11 shows the optimal set of sensors for \$149K. It should be noted that if the number of controlled variables and/or variables for monitoring purposes are changed, the optimal budget is expected to change.

Conclusions

A SND algorithm is developed in this work for maximizing plant efficiency using an estimator-based control system while estimating other variables of interest for a given sensor network budget. We have considered two solution approaches for the SND problem. A concise description is presented for the simultaneous solution approach that can be used for small-scale processes with a few unit operations. A sequential approach is developed for solving the SND problem for large scale, highly integrated plants. In this approach, the GA is used to solve the IP problem while the NLP problem is solved using a tear-stream approach. The direct substitution method is used to solve the "tear stream" in the estimator-based control system. The SND algorithm is then implemented for a highly integrated AGR unit as part of an IGCC power plant with precombustion CO_2 capture. For solving this large-scale problem, a MATLAB® cluster is used for parallel computation leading to significant reduction in computation time. The results shows that as the budget for sensors increases, the number of sensors used and the plant efficiency achieved both increase until a threshold is reached beyond which the budget has minimal impact on plant efficiency. The study also shows that an estimation error in the primary controlled variables, when selected from an economic perspective, can lead to loss in efficiency. However, a further decrease in estimation error below a certain threshold is wasteful as the sensor network budget increases while having minimal impact on the plant efficiency. This SND algorithm is currently developed for grassroots plants, but can be readily enhanced for retrofitting.

Acknowledgment

As part of the National Energy Technology Laboratory's Regional University Alliance (NETL-RUA), a collaborative initiative of the NETL, this technical effort was performed under the RES contract DE-FE0004000.

Notation

A = process transition matrix
a = power consumption coefficient due to solvent regeneration
B = input matrix
b = scalar budget, \$
C = measurement matrix
c_i = cost of individual sensor, \$
F = flow rate, mol/h
Gen = number of generations in GA
K = steady-state Kalman gain matrix
K_c = proportional gain of P-only controller
K_p = steady-state process gain
l = no. of total measurements
m = no. of inputs
N = no. of individuals in population of each generation in GA
N_c = prespecified number of counter
N_s = union set of measured variables
n = number of states
P = pressure
P = state error variance-covariance matrix
$P_c(x_{act})$ = consumed power, MWh
Q = process noise variance-covariance matrix
R = measurement noise variance-covariance matrix
T = temperature
W = weighting factor
t = time, h
u = input
u_{cont} = control input
u_d = disturbance
v = measurement noise vector
w = process noise vector
$\hat{x}$ = vector of estimated states
x_{act} = vector of actual states
x_{CO_2} = composition of CO_2 in liquid phase
y = vector of noisy measurements
$\hat{y}$ = vector of estimated variables
y_{CO_2} = composition of CO_2 in vapor phase
α = time delay, min
β = Decision variable vector of binary numbers (0 and 1)
$\varepsilon(t)$ = deviation of the controlled variable from set point
τ = process time constant, min

Subscripts

act = actual variable
cont = control action
cont, est = estimated controlled variable
$\mathrm{cont_{new}}$ = new control action
CO_2 = carbon dioxide
est = estimated variable
in = inlet or input
max = maximum
ma = process monitoring variables and active constraints
mon, est = monitoring variables calculated from estimated state
N_2 = nitrogen
opt = optimum
out = outlet or, output
set = desired set point
solvent = selexol solvent
$(.)_i$ = ith tray

Literature Cited

1. Bagajewicz M. *Process Plant Instrumentation: Design and Upgrade*. Boca Raton, FL: CRC press, 2000.
2. Raghuraj R, Bhushan M, Rengaswamy R. Locating sensors in complex chemical plants based on fault diagnostic observability criteria. *AIChE J*. 1999;45:310–322.
3. Bhushan M, Rengaswamy R. Design of sensor network based on the signed directed graph of the process for efficient fault diagnosis. *Ind Eng Chem Res*. 2000;39:999–1019.
4. Bhushan M, Rengaswamy R. Comprehensive design of a sensor network for chemical plants based on various diagnosability and reliability criteria. 1. Framework. *Ind Eng Chem Res*. 2002;41(7):1826–1839.
5. Bhushan M, Rengaswamy R. Comprehensive design of a sensor network for chemical plants based on various diagnosability and reliability criteria. 2. Applications. *Ind Eng Chem Res*. 2002;41: 1840−1860.
6. Bhushan M, Narasimhan S, Rengaswamy R. Robust sensor network design for fault diagnosis. *Comput Chem Eng*. 2008;32:1067–1084.
7. Musulin E, Bagajewicz M, Nougues JM, Puigjaner L. Instrumentation design and upgrade for principal components analysis monitoring. *Ind Eng Chem Res*. 2004;43:2150–2159.
8. Narasimhan S, Rengaswamy R. Quantification of performance of sensor networks for fault diagnosis. *AIChE J*. 2007;53:902–917.
9. Bagajewicz M, Cabrera E. New MILP formulation for instrumentation network design and upgrade. *AIChE J*. 2002;48:2271−2282.
10. Bagajewicz M. Design and retrofit of sensor networks in process plants. *AIChE J*. 1997;43(9):2300–2306.
11. Bagajewicz M, Sanchez M. Cost-optimal design of reliable sensor networks. *Comput Chem Eng*. 2000;23(11–12):1757–1762.
12. Chmielewski DJ, Palmer T, Manousiouthakis V. On the theory of optimal sensor placement. *AIChE J*. 2002;48:1001–1012.
13. Kelly JD, Zyngier D. A new and improved MILP formulation to optimize observability, redundancy and precision for sensor network problems. *AIChE J*. 2008;54:1282–1291.
14. Kretsovalis A, Mah RS. Effect of redundancy on estimation accuracy in process data reconciliation. *Chem Eng Sci*. 1987;42:2115–2121.
15. Kadu SC, Bhushan M, Gudi R. Optimal sensor network design for multirate systems. *J Process Control*. 2008;18(6):594–604.
16. Madron F, Veverka V. Optimal selection of measuring points in complex plants by linear models. *AIChE J*. 1992;38:227–236.
17. Ali Y. *Sensor Network Design for Maximizing Reliability of Chemical Processes*. Ph.D. Thesis, Indian Institute of Technology Kanpur, India, 1993.
18. Ali Y, Narasimhan S. Sensor network design for maximizing reliability of linear processes. *AIChE J*. 1993;39:820–828.
19. Ali Y, Narasimhan S. Redundant sensor network design for linear processes. *AIChE J*. 1995;41(10):2237–2249.
20. Peng JK, Chmielewski DJ. Covariance based hardware selection part 2: simultaneous sensor and actuator selection. *IEEE Trans Control Syst Technol*. 2006;14(2):362–368.
21. Peng JK, Chmielewski DJ. *Optimal Sensor Network Design Using the Minimally Backed-Off Operating Point Notion of Profit*. In: Proceedings of the American Control Conference. 2005:220−224.
22. Bagajewicz M, Markowski M. *Instrumentation Design and Upgrade Using an Unconstrained Method with Pure Economical Objectives*. In: Proceedings Foundations of Computer Aided Process Operations. FL: Coral Springs, 2003.
23. Bagajewicz M, Markowski M, Budek A. Economic value of precision in the monitoring of linear systems. *AIChE J*. 2005;51(4):1304–1309.
24. Bagajewicz M. On the definition of software accuracy in redundant measurement systems. *AIChE J*. 2005;51(4):1201–1206.
25. Bagajewicz M. *On a New Definition of a Stochastic-Based Accuracy Concept of Data Reconciliation-Based Estimators*. In: Proceedings

of the 15th European symposium on computer-aided process engineering. 2005.
26. Bagajewicz M. Value of accuracy in linear systems. *AIChE J*. 2006; 52(2):638–650.
27. Bagajewicz M, Nguyen D. Stochastic-based accuracy of data reconciliation estimators for linear systems. *Comput Chem Eng*. 2008; 32(6):1257–1269.
28. Nabil M, Narasimhan S. Sensor network design for optimal process operation based on data reconciliation. *Ind Eng Chem Res*. 2012;51: 6789–6797.
29. Nguyen D, Bagajewicz M. Design of nonlinear sensor networks for process plants. *Ind Eng Chem Res*. 2008;47:5529–5542.
30. Nguyen D, Bagajewicz M. Efficient approximate methods for the design and upgrade of sensor networks. *Ind Eng Chem Res*. 2013;52: 83–90.
31. Meyer M, Le Lann J, Koehret B, Enjalbert M. Optimal selection of sensor location on a complex plant using a graph oriented approach. *Comput Chem Eng*. 1994;18:535–540.
32. Luong M, Maquin D, Huynh C, Ragot J. *Observability, Redundancy, Reliability and Integrated Design of Measurement Systems*. In: Proceeding of 2nd IFAC Symposium on Intelligent Components and Instrument Control Applications. Budapest, Hungary, 1994:8–10.
33. Zumoffen D, Basualdo M. A systematic approach for the design of optimal monitoring systems for large scale processes. *Ind Eng Chem Res*. 2010;49:1749–1761.
34. Carnero M, Hernandez J, Sanchez M, Bandoni A. An evolutionary approach for the design of nonredundant sensor networks. *Ind Eng Chem Res*. 2001;40:5578–5584.
35. Carnero M, Hernandez J, Sanchez M, Bandoni A. On the solution of the instrumentation selection problem. *Ind Eng Chem Res*. 2005;44: 358–367.
36. Sen S, Narasimhan S, Deb K. Sensor network design of linear processes using genetic algorithms. *Comput Chem Eng*. 1998;22:385–390.
37. Lee AJ, Diwekar UM. Optimal sensor placement in integrated gasification combined cycle power systems. *Appl Energy*. 2012;99:255–264.
38. Nguyen D, Bagajewicz M. New sensor network design and retrofit method based on value of information. *AIChE J*. 2011;57:2136–2148.
39. Skogestad S. Control structure design for complete chemical plants. *Comput Chem Eng*. 2004;28:219–234.
40. Jones D, Bhattacharyya D, Turton R, Zitney SE. Plant-wide control system design: primary controlled variable selection. *Comput Chem Eng*. 2014;71;220–234.
41. Skogestad S. Plantwide control: the search for the self-optimizing control structure. *J Process Control*. 2000;10(5):487–507.
42. Figueroa JD, Fout T, Plasynski S, McIlvried H, Srivastava R. Advances in CO_2 capture technology—The U.S Department of Energy's Carbon Sequestration Program. *Int J Greenhouse Gas Control*. 2008;2:9–20.
43. Kalman RE, Bucy RS. New results in linear filtering and prediction theory. *J Basic Eng*. 1961;83(3):95–108.
44. Haupt RL, Haupt SE. *Practical Genetic Algorithms*, 2nd ed. New Jersey: Wiley-Interscience, 2004.
45. Bhattacharyya D, Turton R, Zitney SE. Steady-state simulation and optimization of an integrated gasification combined cycle (IGCC) power plant with CO_2 capture. *Ind Eng Chem Res*. 2011;50:1674–1690.
46. Carter LD. An early deployment strategy for carbon capture, utilization, and storage (CCUS) technologies. United States Carbon Sequestration Council. June, 2012, Available at: http://www.uscsc.org/Files/Admin/Educational_Papers/20120604_Early Deployment Strategy for CCUS Technologies_FINAL.pdf, Last accessed October 17, 2014.
47. Ziegler JG, Nichols NB. Optimum setting for automatic controllers. *Trans ASME*. 1942;64:759–768.
48. Cohen GH, Coon GA. Theoretical considerations of retarded control. *Trans ASME*. 1953;75:827–834.
49. Ogunnaike BA, Ray WH. Process Dynamics, Modeling and Control. New York: Oxford University press, 1994;536–537.
50. Liptak BG. *Process Measurement and Analysis*, *4th ed*. Boca Raton, FL: CRC press, 2003.

Manuscript received July 17, 2014, and revision received Sep. 22, 2014.